Shape Diagram of Vesicles in Poiseuille Flow

Gwennou Coupier,[1,*] Alexander Farutin,[1] Christophe Minetti,[2] Thomas Podgorski,[1] and Chaouqi Misbah[1]

[1]*Laboratoire Interdisciplinaire de Physique, CNRS et Université J. Fourier-Grenoble I, BP 87, 38402 Saint-Martin d'Hères, France*

[2]*Microgravity Research Center, Université Libre de Bruxelles, 50 Avenue F. Roosevelt, B-1050 Brussels, Belgium*

(Received 26 October 2011; published 25 April 2012)

Soft bodies flowing in a channel often exhibit parachutelike shapes usually attributed to an increase of hydrodynamic constraint (viscous stress and/or confinement). We show that the presence of a fluid membrane leads to the reverse phenomenon and build a phase diagram of shapes—which are classified as bullet, croissant, and parachute—in channels of varying aspect ratio. Unexpectedly, shapes are relatively wider in the narrowest direction of the channel. We highlight the role of flow patterns on the membrane in this response to the asymmetry of stress distribution.

DOI: 10.1103/PhysRevLett.108.178106 PACS numbers: 87.16.D−, 83.50.Ha

The shape of soft bodies under flow is governed by strong nonlinear coupling between hydrodynamic stresses and elastic restoring forces. The latter are often linked with specific interface properties, like surface tension, or bending and shear elasticity of an elastic or liquid membrane.

A widely studied flow is the confined Poiseuille flow, in which the behavior of red blood cells (RBCs) [1–4], drops [5–7], lipid vesicles [3,4,8–10], capsules [11–16], or polymers [17] is often considered. Underlying motivations include a better understanding of blood flow or the possibility to manipulate these objects in microfluidic devices for lab on chip applications. The most commonly reported stationary shapes are axisymmetric bulletlike and parachutelike shapes, the latter being characterized by a concave rear part. The shape of this rear part is very sensitive to the mechanical environment; therefore, observing it is a (cheap) rheology experiment in itself, as exemplified in Refs. [12,13], where possible membrane constitutive laws for capsules are discussed. Similarly, in Ref. [14], the onset of curvature inversion is shown to be strongly dependent on the capsule's prestress.

Alternatively, this shape will give indications on the hydrodynamic stresses on the object. It is generally observed that increasing the flow velocity, or the confinement, leads first to an increase in the fore-aft asymmetry, then to the apparition of a negative curvature region at the rear, and eventually, at least for membraneless objects, to breakup. Hydrodynamic interactions between neighboring objects are also strongly correlated to shape-dependent modifications of the local flow. In Ref. [4], small clusters of RBCs are simulated, and two well separated states (compact or loose clusters) are explicitly associated with two different cell shapes (shallow or deep parachute). This hydrodynamic cell aggregation is mediated by a loop of fluid recirculation between cells, also called a bolus [2,3,18], whose apparition or disappearance is intimately correlated with shape changes [4]. Thus, understanding the conditions for the apparition and stability of shapes and the resulting flow patterns around them provides a valuable entry point to build up hydrodynamic aggregation rules in a suspension. At larger scale, this self-organization of the suspension leads to specific rheological properties like the shear thinning of blood or the Fårhæus-Lindquist effect [19]. Even in the case of an isolated cell in a dilute suspension, shape variations will modify viscous dissipation and, therefore, the effective viscosity of the suspension. Again, specific changes in this viscosity can be associated with concavity changes at the rear and loss of membrane tension [8].

In this Letter, we identify shape changes with flow variations in the case of fluid vesicles, which are also simplified models for RBCs. We shall see that the general and therefore intuitive sketch of concavity increase with hydrodynamic stress must be reconsidered in the case of vesicles, which differ from drops or capsules by their inextensible fluid membranes. We study explicitly the effect of three flow characteristics: its velocity, the confinement, and its axial asymmetry.

The problem is considered through experiments, numerical simulations, and theoretical calculations. In the experiments, we use a polydimethylsiloxane microfluidic device. Vesicles are prepared by following the standard electroformation method, which produces vesicles of various size and deflation. They are made of a dioleoylphosphatidylcholine lipid bilayer enclosing an inner solution of sugar in water. Vesicles are then diluted in another sugar solution and imaged by phase contrast microscopy. The viscosity ratio between both solutions is close to unity. Vesicles flow along the x axis in a straight channel of constant thickness d_z (z direction) and varying width d_y (y direction). Their cross section in the xy plane is observed (Fig. 1). Gravity is in the x direction, so that quick centering is achieved [10]. Each section of given width is long enough for stationary shapes to be reached. The analytical calculation is based on the decomposition of the shape in spherical harmonics. For simplicity, we neglect the influence of channel walls and use for the velocity profile $v(y, z) = V[1 - (2y/d_y)^2 - (2z/d_z)^2]$, which turns out to

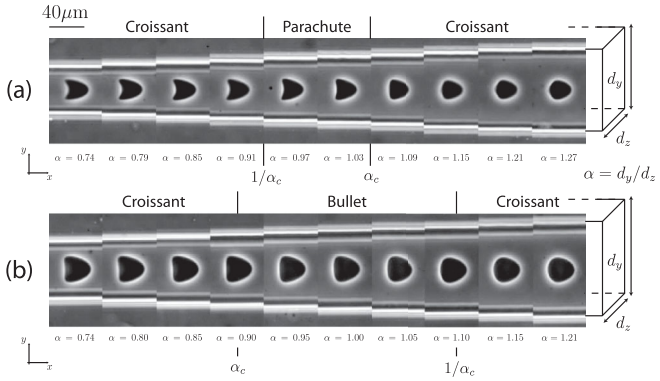

FIG. 1. Vesicle cross sections in a channel of increasing aspect ratio. (a) $\nu = 0.913$, $\hat{R} = 0.35$, and $C_a = 59$. (b) $\nu = 0.973$, $\hat{R} = 0.38$, and $C_a = 81$. $\hat{R}$ and C_a are given for the square section.

be a valid approximation for low confinements. As in Ref. [20], solving the Stokes equations together with the boundary conditions at the membrane and at infinity and using the condition of stationary shape, we find expressions for the amplitude of each considered harmonic as a function of ν, C_a, and α. This method is much more efficient than the traditional one, which is based on derivation and numerical solution of the shape evolution equations [21]. We can now take 18 harmonics for the axisymmetric case and 12 for elliptic cross sections. The accuracy of the results was verified by 3D numerical simulations using the boundary integral method [22]. Finding theoretical and numerical approaches that fit the experimental results up to the shape details is still a challenging issue, as illustrated by the acute debate around phase diagrams of vesicles under shear flow [22,23]. Here, we find excellent agreements, as exemplified by the superimposition of shapes in Fig. 2.

Fluid vesicles have constant volume and surface area. Their deformability is directly linked to their initial (and constant) deflation, given by the reduced volume $\nu = \mathcal{V}/[4\pi(\mathcal{S}/4\pi)^{3/2}/3]$, where $\mathcal{V}$ and $\mathcal{S}$ are the vesicle volume and membrane area, respectively. In the experiments, both are calculated thanks to axial symmetry of the shape in the square cross-section channel, on which we comment later. The typical size of a vesicle is given by its

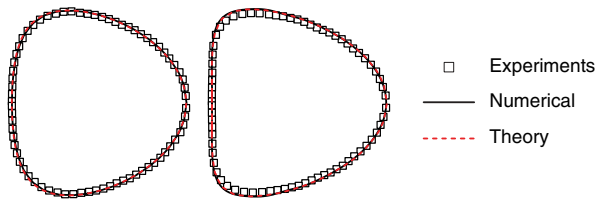

FIG. 2 (color online). Cross sections for two vesicles in symmetric flow (experiment, $\hat{R} = 0.38$; simulation and theory, $\hat{R} = 0$). Left, $\nu = 0.979$ and $C_a = 4191$; right, $\nu = 0.946$ and $C_a = 3776$. No fitting parameters.

effective radius $R = \sqrt{\mathcal{S}/4\pi}$. The geometry of the problem is characterized by two dimensionless numbers: the channel aspect ratio $\alpha = d_y/d_z$ and the confinement $\hat{R} = 2R/\sqrt{d_y d_z}$. The capillary number, that compares viscous stress to membrane elasticity, is defined by $C_a = V/(d_y d_z)R^4\eta/\kappa$, where V is the unperturbed fluid maximum velocity, η the fluid viscosity, and κ the membrane bending modulus.

Overall, the problem is described by the four dimensionless parameters (ν, α, $\hat{R}$, and C_a). The explored ranges are summarized in Table I.

Preliminary observation.—When vesicles flow from narrow to wide sections (the thickness d_z being constant), their in-plane section becomes less asymmetric between the front and the rear, and the negative curvature region at the rear, if any, disappears (Fig. 1). The 2D shapes are symmetric about the Ox axis [24]. A given vesicle flowing several times back and forth in the square channel always shows the same 2D shape, which indicates that it adopts, at least, the square symmetry. Thanks to digital holographic microscopy, we have recently seen that the vesicle's transverse cross sections are elliptical [26]. We then reach the *a priori* nontrivial conclusion that the vesicle shape obeys axial symmetry in a square geometry. We observe two types of axisymmetric shapes, namely, parachute and bullet. We first investigate their existence domains in the symmetric channel ($\alpha = 1$) and then explore the influence of asymmetry for low constraints ($\hat{R} \leq 0.5$, $C_a \lesssim 500$).

Effect of C_a and $\hat{R}$ in the symmetric channel.—For weakly confined vesicles ($\hat{R} \leq 0.5$), clear separation between the bullet and parachute domains is achieved in the (ν, C_a) space, although $\hat{R}$ varies by a factor of 4 [Fig. 3(a)]. A completely unexpected observation is the crossover from parachute to bullet by increasing C_a for vesicles with a reduced volume between 0.95 and 0.97. The same trend is theoretically observed for unbounded flow. The full 3D simulations support these results. We observe, however, a slight shift in C_a between experiments and theory. This could be attributed to uncertainties on the bending modulus (not measured) and to effects of thermal fluctuations and confinement, which were neglected in the theory. We have checked that taking into account a possible spontaneous curvature of the membrane has only a minor effect on the results.

While, for weak confinement ($\hat{R} \leq 0.5$), the parachute to bullet crossover depends on the capillary number but not on the confinement, the situation is completely opposite for

TABLE I. Parameter ranges. For the experiments, $\eta = 10^{-3}$ Pa · s, $\kappa = 10^{-19}$ J, and $V \in [10; 8300]$ μm · s^{-1}.

	ν	α	$\hat{R}$	C_a
Experiments	0.910–1	0.49–1.74	0.12–1.27	$3 - 7 \times 10^4$
Theory	0.9–1	0.5–2	0	$10 - 6 \times 10^4$

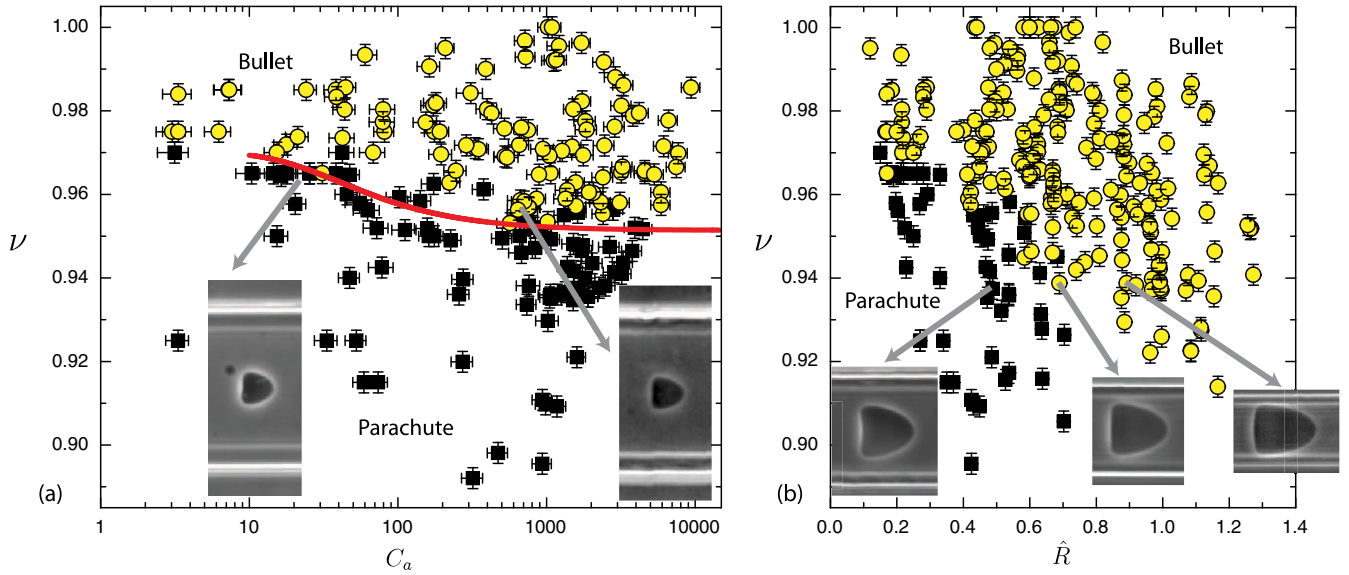

FIG. 3 (color online). Shapes for $\alpha = 1$. Dots refer to experimental data and the full line to theory and simulations. (a) Bullet-parachute phase diagram in the (ν, C_a) plane for not too confined vesicles ($0.12 \leq \hat{R} \leq 0.5$). Pictures in the inset ($\nu = 0.964$, $\hat{R} = 0.24$, $C_a = 20$ and $\nu = 0.959$, $\hat{R} = 0.25$, $C_a = 667$) illustrate the concavity change as C_a increases. (b) Bullet-parachute phase diagram in the $(\nu, \hat{R})$ plane. For $\hat{R} \geq 0.4$, C_a goes from 15 to 70 000, while for $\hat{R} \leq 0.4$, values are limited to the $C_a < 100$ range due to shape dependency on C_a in the unbounded case. Pictures in the inset ($\nu = 0.938$ and $\hat{R} = 0.49$, 0.69, and 0.89) illustrate the concavity change as $\hat{R}$ increases.

more confined vesicles. As shown in Fig. 3(b), for $\hat{R} \geq 0.5$, well separated domains are found in the $(\nu, \hat{R})$ plane, despite the strong variations of C_a (more than three decades). This indicates that when confinement is large enough, its effect is dominant. Contrary to the intuition, the bullet shape is favored upon an increase of confinement.

Effect of asymmetry.—We observed that, for a vesicle of given reduced volume ν, the 2D cross section and, in particular, the concavity are independent of $\hat{R}$ and C_a for low constraint ($\hat{R} \leq 0.5$, $C_a \lesssim 500$) and depend only on asymmetry α [27]. Because of this $(\hat{R}, C_a)$ independence, the full 3D shape of a vesicle under flow of aspect ratio α is deduced from its two in-plane shapes in the sections of aspect ratios α and $1/\alpha$, where $\hat{R}$ and C_a are different. For instance, in Fig. 1(a), the shapes in sections $\alpha = 0.79$ and $\alpha = 1.27 \simeq 1/0.79$ can be seen as the top and side views of the same vesicle in a rectangular channel of aspect ratio 0.79. We define α_c as the aspect ratio of the channel where the crossover from concave to convex 2D shape occurs. If α_c is larger than 1, as in Fig. 1(a), then, for $1 \leq \alpha < \alpha_c$, the in-plane cross section of the vesicle is concave, and its orthogonal cross section, for which we consider $1/\alpha < \alpha_c$, is also concave. The 3D shape is therefore a parachute. If $\alpha \geq \alpha_c$, the in-plane shape is convex, while the orthogonal shape is concave, since $1/\alpha \leq \alpha_c$. Such a "croissant" shape has been seen for drops between two infinite planes [6]. If α_c is lower than 1, as in Fig. 1(b), the same reasoning shows that the 3D shape is a bullet for $1 \leq \alpha \leq 1/\alpha_c$ and a croissant for $\alpha > 1/\alpha_c$. Some weakly deflated vesicles show no concave shape in the explored α range and are, therefore, always bullets. Combining all these data, we deduce the general phase diagram in the (ν, α) space (Fig. 4, restricted to $\alpha \geq 1$ for symmetry reasons), which is in good agreement with the theory for $\hat{R} = 0$ and low C_a. For $\alpha = 1$, one gets a parachute or a bullet shape; increasing the asymmetry of the channel leads to the croissant shape, which has a concave part in the plane of higher stress.

Discussion and conclusion.—We reported the phase diagram of vesicle shapes in Poiseuille flow in the relevant parameter space. Our study reveals the necessity to distinguish between isotropic and anisotropic variations of the

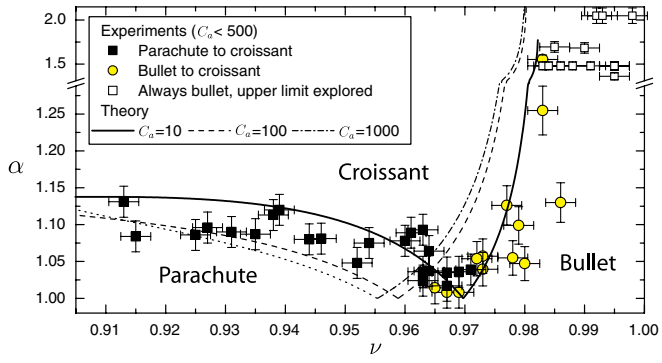

FIG. 4 (color online). Shape diagram in asymmetric channel at low constraint. Experiment: Each point corresponds to a vesicle with $\hat{R} \leq 0.5$ and $C_a \lesssim 500$ when $\alpha = 1$. Theory: $\hat{R} = 0$ and $C_a \leq 1000$.

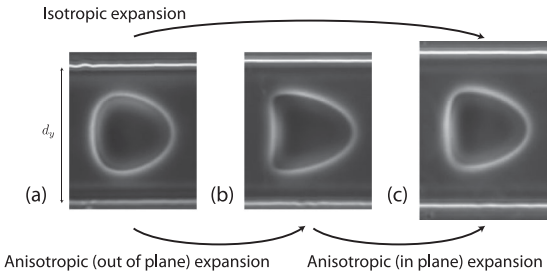

FIG. 5. Cross sections for the same vesicle ($\nu = 0.985$) in three channels. (a) $d_y = d_z = 83$ μm; (b) $d_y = 83$ μm, $d_z = 92$ μm; (c) $d_y = d_z = 92$ μm. (a) and (b) give indications on what would be seen in the xz plane of Fig. 1(b).

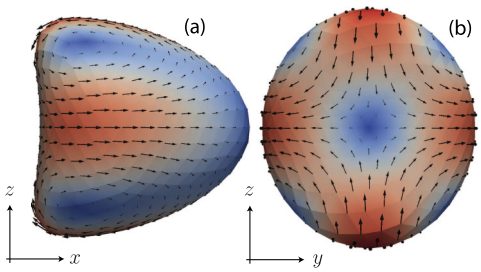

FIG. 6 (color online). Velocity field in the vesicle comoving frame. Side (a) and rear (b) view. Simulations, $\nu = 0.95$, $C_a = 100$, and $\alpha = 1.2$ (croissant shape). The norm of velocity is color-coded. Maximum velocity is about 5 times lower than vesicle velocity. See also [27].

cross section of the channel. While the evolution shown in Fig. 1 is consistent with expectations (increasing confinement leads to more curved shapes), increasing isotropically the confinement leads actually to less curved shapes, as shown by shapes in the inset in Fig. 3(b). The same conclusion is reached if the flow strength is increased at a given confinement. Theoretical and numerical results support these conclusions, for symmetric but also for asymmetric flows: As shown in Fig. 4, the less distorted bullet and croissant shapes are favored against the parachute shape upon increasing flow strength. Figure 5 summarizes our main finding; isotropic expansion [Figs. 5(a) and 5(c)] leads unexpectedly to more shape distortion, while in-plane-only expansion [Figs. 5(b) and 5(c)] leads to a less curved shape. In that case, the asymmetry between the two transverse directions allows us to relax the constraints of perimeter and surface conservation at the level of a given longitudinal cross section, whose evolution is therefore similar to the one of a drop or a capsule. Finally, the predominant role played by the aspect ratio of the channel is illustrated by the concavity increase through out-of-plane-only expansion [Figs. 5(a) and 5(b)], which then appears to be equivalent to an in-plane contraction. The latter case also indicates that a sole 2D view in experiments might lead to biased considerations when discussing the existence of parachutes, as in Ref. [28].

In asymmetric channels, vesicle shapes exhibit another unexpected feature: As seen in Fig. 1 and in Ref. [27], their in-plane width does not increase with d_y but is roughly constant. Therefore, contrary to drops [7], vesicles do not adopt the aspect ratio of the channel but occupy a space in the yz plane that is delimited by a circle. The fact that the fluid then has to go through a small gap in the narrowest width of the channel may lead to the intuitive but wrong conclusion that the vesicle should decrease its extent in that direction (and follow more or less the channel aspect ratio). In order to get an insight on this peculiar phenomenon, we investigated the patterns of membrane surface flow through simulations (Fig. 6). As soon as the channel is asymmetric, 4 vortices appear on the surface with a backward flow in the direction corresponding to the narrowest gap, which decreases the mean shear in the gap and the viscous stress on the membrane. The opposite takes place in the other direction, leading to a more homogeneous stress distribution. When drops adopt the channel cross section, all material points on their surface are advected backward [27]. The corresponding flow line possesses two in-plane stagnation points at the front and at the back, on the main axis. This apparent singularity is resolved for drops through recirculation inside the drop, a fact that is precluded for a membrane whose material points must stay on the surface. This difference has already been underlined for drops and vesicles bounded to a substrate and submitted to shear flow [29]. The 4-vortex pattern is thus the simplest acceptable flow pattern on the vesicle surface, if we consider that zero flow situation is unlikely to happen for this fluid membrane under asymmetric constraint. This pattern can be compared to the one obtained recently for vesicle sedimentation [30]. Despite the axial symmetry of the problem, it is shown that a croissant shape with four vortices on its surface is a possible stationary shape. However, the stability of this solution is not discussed.

Flow asymmetry, which can be due to the channel geometry or to the presence of neighboring cells, will have therefore two consequences: From the rheological point of view, surface vortices of non-negligible velocity (see Fig. 6) imply important motions of the fluid inside the vesicle (or the RBC) that will contribute to the net dissipation. These vortices, that would not be caught, for instance, by 2D simulations, will also affect accordingly the flow field around the membrane, which will modify in return the recirculating loop between cells. Whether this mechanism would be a stabilizing or destabilizing factor in cell clusters, that often exhibit symmetry breaking [3], remains to be discussed.

We acknowledge financial support from CNES and the ANR "MOSICOB project." This work was also supported by the SSTC/ESA-PRODEX (Services Scientifiques Techniques et Culturels/European Space Agency-Programmes de Développement d'expériences) Contract No. 90171.

*gwennou.coupier@ujf-grenoble.fr

[1] R. Skalak and P. I. Branemark, Science **164**, 717 (1969); T. W. Secomb, B. Styp-Rekowska, and A. R. Pries, Ann. Biomed. Eng. **35**, 755 (2007); M. Abkarian, M. Faivre, R. Horton, K. Smistrup, C. A. Best-Popescu, and H. A. Stone, Biomed. Mater. **3**, 034011 (2008); G. Tomaiuolo, M. Simeone, V. Martinelli, B. Rotoli, and S. Guido, Soft Matter **5**, 3736 (2009).

[2] P. Gaehtgens, C. Dührssen, and K. H. Albrecht, Blood Cells **6**, 799 (1980).

[3] J. L. McWhirter, H. Noguchi, and G. Gompper, Proc. Natl. Acad. Sci. U.S.A. **106**, 6039 (2009).

[4] J. L. McWhirter, H. Noguchi, and G. Gompper, Soft Matter **7**, 10967 (2011).

[5] B. P. Ho and L. G. Leal, J. Fluid Mech. **71**, 361 (1975); W. L. Olbricht and D. M. Kung, Phys. Fluids A **4**, 1347 (1992); E. Lac and J. D. Sherwood, J. Fluid Mech. **640**, 27 (2009); S. Guido and V. Preziosi, Adv. Colloid Interface Sci. **161**, 89 (2010).

[6] A. J. Griggs, A. Z. Zinchenko, and R. H. Davis, Int. J. Multiphase Flow **33**, 182 (2007).

[7] F. Sarrazin, T. Bonometti, L. Prat, C. Gourdon, and J. Magnaudet, Microfluid. Nanofluid. **5**, 131 (2008); C. N. Baroud, F. Gallaire, and R. Dangla, Lab Chip **10**, 2032 (2010).

[8] R. Bruinsma, Physica (Amsterdam) **234A**, 249 (1996).

[9] V. Vitkova, M. Mader, and T. Podgorski, Europhys. Lett. **68**, 398 (2004); H. Noguchi and G. Gompper, Proc. Natl. Acad. Sci. U.S.A. **102**, 14 159 (2005).

[10] G. Coupier, B. Kaoui, T. Podgorski, and C. Misbah, Phys. Fluids **20**, 111702 (2008).

[11] F. Risso, F. Collé-Paillot, and M. Zagzoule, J. Fluid Mech. **547**, 149 (2006).

[12] C. Quéguiner and D. Barthès-Biesel, J. Fluid Mech. **348**, 349 (1997).

[13] Y. Lefebvre, E. Leclerc, D. Barthès-Biesel, J. Walter, and F. Edwards-Lévy, Phys. Fluids **20**, 123102 (2008).

[14] Y. Lefebvre and D. Barthès-Biesel, J. Fluid Mech. **589**, 157 (2007).

[15] S. Kuriakose and P. Dimitrakopoulos, Phys. Rev. E **84**, 011906 (2011).

[16] X.-Q. Hu, A.-V. Salsac, and D. Barthès-Biesel, J. Fluid Mech. (to be published).

[17] S. Reddig and H. Stark, J. Chem. Phys. **135**, 165101 (2011).

[18] C. Pozrikidis, Phys. Fluids **17**, 031503 (2005); H. Selmi, L. Elasmi, G. Ghigliotti and C. Misbah, Discrete Contin. Dyn. Syst. **15**, 1065 (2011).

[19] Y. C. Fung, *Biomechanics: Mechanical Properties of Living Tissues* (Springer, Berlin, 1993).

[20] D. Barthès-Biesel, J. Fluid Mech. **100**, 831 (1980).

[21] A. Farutin and C. Misbah, Phys. Rev. E **84**, 011902 (2011).

[22] T. Biben, A. Farutin, and C. Misbah, Phys. Rev. E **83**, 031921 (2011).

[23] J. Deschamps, V. Kantsler, and V. Steinberg, Phys. Rev. Lett. **102**, 118105 (2009); N. J. Zabusky, E. Segre, J. Deschamps, V. Kantsler, and V. Steinberg, Phys. Fluids **23**, 041905 (2011).

[24] Asymmetric slippers are occasionally observed but are not stable. Stability conditions of slipper shapes for vesicles and RBCs are still under debate [1,4,21,25], and we shall not enter into it much further.

[25] B. Kaoui, G. Biros, and C. Misbah, Phys. Rev. Lett. **103**, 188101 (2009).

[26] C. Minetti, N. Callens, G. Coupier, T. Podgorski, and F. Dubois, Appl. Opt. **47**, 5305 (2008).

[27] See Supplemental Material at http://link.aps.org/supplemental/10.1103/PhysRevLett.108.178106 for details of shape changes with channel aspect ratio in the experiments. We also show more velocity fields on the membranes of vesicles and compare them with the case of droplets.

[28] H. Noguchi, G. Gompper, L. Schmid, A. Wixforth, and T. Franke, Europhys. Lett. **89**, 28 002 (2010).

[29] C. Vézy, G. Massiera, and A. Viallat, Soft Matter **3**, 844 (2007); P. Dimitrakopoulos and J. J. L. Higdon, J. Fluid Mech. **336**, 351 (1997).

[30] G. Boedec, M. Jaeger, and M. Leonetti, J. Fluid Mech. **690**, 227 (2012).